MOLECULAR PHARMACOLOGY, 20:404–414

Interaction of the Antitumor Drug 4′-(9-Acridinylamino)methanesulfon-*m*-anisidide and Related Acridines with Nucleic Acids

WILLIAM R. WILSON, BRUCE C. BAGULEY, LAURENCE P. G. WAKELIN, AND MICHAEL J. WARING[1]

Departments of Pathology and Cell Biology, University of Auckland, Auckland, New Zealand, and Department of Pharmacology, University of Cambridge Medical School, Cambridge CB2 2QD, England

Received December 29, 1980; Accepted May 26, 1981

SUMMARY

WILSON, W. R., B. C. BAGULEY, L. P. G. WAKELIN, AND M. J. WARING. Interaction of the antitumor drug 4′-(9-acridinylamino)methanesulfon-*m*-anisidide and related acridines with nucleic acids. *Mol. Pharmacol.* **20**:404–414 (1981).

The acridine antitumor drug 4′-(9-acridinylamino)methanesulfon-*m*-anisidide (*m*-AMSA), which is currently in Phase II clinical trial, is known to be an inhibitor of nucleic acid synthesis. The intercalative binding of this drug to native calf thymus DNA has been studied using equilibrium dialysis, spectrophotometry, and competition with ethidium. All three techniques indicate an intrinsic association constant of approximately 1.5 $\times 10^5$ M^{-1} at an ionic strength of 0.01. The binding isotherm is adequately described by a neighboring-site exclusion model, and indicates a site size of approximately two base pairs. At elevated ionic strength the association constant is depressed by a factor which corresponds closely to that predicted for a monocationic ligand. Studies with a variety of synthetic polynucleotides indicate that association constants for binding sites of different sequence vary over a 10-fold range. *m*-AMSA binds to heat-denatured calf thymus DNA or ribosomal RNA with association constants, respectively, 5- and 25-fold lower than that for native DNA. Comparable measurements have been made with related acridinylaminomethanesulfonanilide (AMSA) drugs and simple aminoacridines; they reveal that the presence of an unsubstituted methanesulfonanilide ring does not noticeably interfere with binding to native DNA. However, addition of a methoxy substituent at the 3′ position of this ring, as in *m*-AMSA, may sterically hinder intercalation of the acridine nucleus of the drug. The antitumor activity of the series of ligands studied could not be correlated in any straightforward fashion with nucleic acid binding parameters, although the conspicuous ability of AMSA drugs to discriminate sensitively between native DNA and RNA may result in efficient binding to DNA *in vivo*.

INTRODUCTION

m-AMSA[2] is an acridine drug that shows broad spectrum activity against experimental tumors in animals (1, 2) and is being evaluated at present for antitumor activity in Phase II clinical trials. It appears to possess clinical activity of an order similar to that of adriamycin in the treatment of acute leukemia[3] and advanced breast cancer (3).

m-AMSA was first synthesized and tested for antitumor activity by Cain *et al.* (4) as part of a systematic drug development program which has now generated several hundred analogues of this drug (ref. 5 and references therein). The development of this AMSA series was predicated on the assumption that the acridine moiety of these drugs allows intercalative DNA binding and that this binding is required for antitumor activity. Con-

This investigation was supported by the Auckland Division of the Cancer Society of New Zealand, the Medical Research Councils of New Zealand and Great Britain, the Royal Society, and the Cancer Research Campaign.

[1] Supported by a Wellcome-New Zealand Medical Research Council Research Travel Grant.

[2] The abbreviations used are: *m*-AMSA, 4′-(9-acridinyl-amino)-methanesulfon-*m*-anisidide; AMSA, 4′-(9-acridinyl-amino)methanesulfonanilide; *o*-AMSA, 4′-(9-acridinyl-amino)methanesulfon-*o*-anisidide; 2-Me-AMSA, 4′-(2-methyl-9-acridinylamino)methanesulfonanilide; 9-AA, 9-aminoacridine; 9-Me-AA, 9-methylaminoacridine; TYMV, turnip yellow mosaic virus; MAF buffer, buffer containing 9.25 mM NH_4F, 2 mM 2-[*N*-morpholino]ethanesulfonic acid, and 10 μM EDTA and adjusted to pH 6.0 with ammonia solution (final ionic strength 0.01). DMSO, dimethyl sulfoxide; SHE buffer, buffer containing 9.4 mM NaCl, 2 mM 4-(2-hydroxyethyl)1-piperazine-ethanesulfonic acid, and 20 μM EDTA and adjusted to pH 7.0 with NaOH (final ionic strength 0.01).

[3] Information presented at the Sixteenth Meeting of the American Society for Clinical Oncology, San Diego, Calif. (1980).

0026-895X/81/020404-11$02.00/0

sistent with this hypothesis (while by no means establishing it), *m*-AMSA produces several effects in tumor cells which appear likely to result from interference with DNA structure or metabolism: selective inhibition of DNA synthesis (6), inhibition of chromosome condensation in late G_2-phase (6, 7), formation of single-strand breaks (or alkali-labile sites) in DNA (6, 8), and generation of a variety of chromosomal aberrations (9). Physical binding of *m*-AMSA to DNA *in vitro* has been demonstrated by spectrophotometric titration (6, 10), equilibrium dialysis (10), competition between ethidium and *m*-AMSA for DNA sites (11), and by hydrodynamic studies with closed circular duplex DNA (12), the latter establishing an intercalative mode of binding.

In this study we have used a variety of physical techniques to examine the binding of *m*-AMSA and related compounds to nucleic acids. In order to establish whether the methanesulfonanilide ring of *m*-AMSA, which probably lies almost orthogonal to the plane of the acridine nucleus (13), influences the interaction we have compared the binding of AMSA drugs and simpler acridines (9-aminoacridine, 9-methylaminoacridine, proflavine). The drugs studied (Fig. 1; Table 1) include *m*-AMSA; the parent compound (AMSA), which is also active against experimental tumors but is less potent (14); *o*-AMSA, an inactive positional isomer of *m*-AMSA (5); and 2-Me-AMSA, which is also inactive against tumors (14) and may bind to DNA with different geometry, since it produces a lower unwinding angle than do the other three AMSA drugs (12).

Having regard to the selectivity of these drugs *in vivo* we have sought to examine any possible correlation between their binding to different nucleic acids and their biological activity, and to relate the observations to molecular structure where feasible.

MATERIALS AND METHODS

Ligands. AMSA drugs were synthesized by Professor B. F. Cain, the Cancer Chemotherapy Laboratory, University of Auckland, (Auckland, New Zealand), and were supplied by him in the form of anhydrous methanesulfonate salts. Dr. R. G. McR. Wright, Oxford University (Oxford, England) purified and provided proflavine and 9-AA as the hydrated hydrochloride salts. The anhydrous hydrochloride salt of 9-Me-AA was a gift from Dr. E. S. Canellakis, Yale University (New Haven, Conn.). All ligands obeyed Beer's law over the concentration range of interest. Extinction coefficients are given in Table 1.

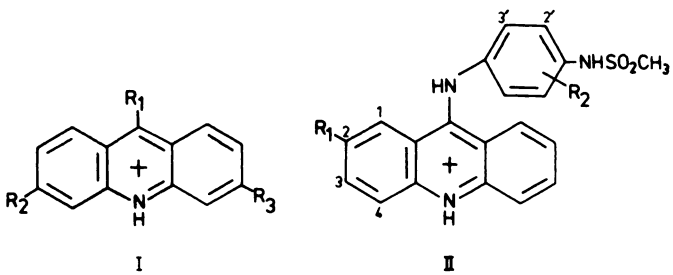

FIG. 1. *Structural formulae of acridine derivatives studied (see Table 1)*

These values were used to determine the concentration of drug in fresh aqueous stock solutions which were prepared by dissolving in buffer at room temperature and filtering to remove undissolved material.

Nucleic acids. Calf thymus DNA (Type V, sodium salt) was purchased from Sigma Chemical Company (St. Louis, Mo.) and wheat germ ribosomal RNA (sodium salt) from Calbiochem (San Diego, Calif.). TYMV RNA was a gift from Professor R. K. Ralph, Department of Cell Biology, University of Auckland. Poly(dA-dG)·poly(dC-dT) was kindly provided by Professor A. R. Morgan, Department of Biochemistry, University of Alberta (Edmonton, Alberta, Canada). All other synthetic polynucleotides were obtained from Boehringer Mannheim, (Mannheim, Federal Republic Germany), with the exception of poly(dA-dT), which was obtained from Miles Research Products (Elkhart, Ind.). Nucleic acid solutions were dialyzed exhaustively against the appropriate buffer and stored at −20°. Immediately before use these solutions were thawed, centrifuged to remove particulate matter (10,000 × *g* for 30 min at 40°), and the nucleic acid concentration was determined by spectrophotometry. Extinction coefficients were taken from ref. 15 (synthetic DNAs), ref. 16 (calf thymus DNA), ref. 17 (TYMV RNA), or the suppliers' data (rRNA). Denatured DNA was prepared immediately prior to use by heating native DNA at 95–98° for 2 min and cooling rapidly on ice. The extinction coefficient of heat-denatured calf thymus DNA in MAF buffer was 8270 M^{-1} cm^{-1} at 260 nm. All nucleic acid concentrations are expressed in terms of molarity with respect to nucleotide residues.

Equilibrium dialysis. Binding curves were measured by equilibrium dialysis using an MSE Dianorm apparatus. Dialysis cells having two 5-ml compartments separated by a Spectrapor 2 regenerated cellulose membrane (nominal mol wt cutoff 12,000–14,000) were loaded with approximately 4 ml of 152 or 455 μM nucleic acid in MAF buffer in one chamber and the same volume of the appropriate drug solution in the other. The cells were rotated at 12 rpm in a water bath at 25° for 20–24 hr, although equilibrium was routinely attained within 3–4 hr. At equilibrium the drug concentration in each chamber was determined spectrophotometrically using either 40 mm or 10 mm light-path quartz semimicrocuvettes depending on the magnitude of the optical density. For the free drug side, the extinction coefficients determined in MAF buffer listed in Table 1 were used; for the other side the complex was dissociated by addition of an equal volume of DMSO with or without acetic acid to yield a final concentration of 0.5% (v/v) (18), and the total drug concentration was estimated using the molar extinction-coefficients of 50% DMSO-buffer mixtures also given in Table 1. Appropriate controls were performed to verify complete dissociation of the nucleic acid complexes by DMSO over the entire range of binding levels studied.

Spectrophotometric titrations. The visible absorption spectrum (350–580 nm) was determined at 23–26° for each ligand in the presence of varying concentrations of nucleic acid, using a Cary 15 recording spectrophotometer. The sample cuvette (path length 10 mm) contained the test drug in SHE buffer. To this was added a small volume of a concentrated nucleic acid solution in the

TABLE 1

Nomenclature and spectral characteristics of ligands

Structure (Fig. 1)	Abbreviation	MAF buffer		50% DMSO in MAF		SHE buffer	
		λ^a	$10^{-3} \times \epsilon^b$	λ^a	$10^{-3} \times \epsilon^b$	λ^a	$10^{-3} \times \epsilon^b$
		nm	$M^{-1}\ cm^{-1}$	*nm*	$M^{-1}\ cm^{-1}$	*nm*	$M^{-1}\ cm^{-1}$
I; $R_1 = NH_2$ $R_2 = R_3 = H$	9-AA	398	10.0	403	10.9	400	9.82
I; $R_1 = NHCH_3$ $R_2 = R_3 = H$	9-Me-AA	404	11.0	408	10.9		
I; $R_1 = H$ $R_2 = R_3 = NH_2$	Proflavine	445	40.7	455	53.0		
II; $R_1 = R_2 = H$	AMSA	435[c]	13.1[c]	433	11.6	433	12.4
				438[d]	13.1[d]		
II; $R_1 = H$ $R_2 = 2'\text{-}OCH_3$	*o*-AMSA	435[c]	13.5[c]	433	11.2	433	12.1
				438[d]	12.9[d]		
II; $R_1 = H$ $R_2 = 3'\text{-}OCH_3$	*m*-AMSA	435[c]	14.2[c]	433	11.8	434	12.0
				438[d]	14.5[d]		
II; $R_1 = CH_3$ $R_2 = H$	2-Me-AMSA	438[c]	12.8[c]	436	11.8		
				440[d]	12.6[d]		

[a] Wavelength of maximal visible absorbance.
[b] Extinction coefficient at wavelength λ.
[c] In the presence of 0.5% (v/v) DMSO.
[d] In the presence of 0.5% (v/v) acetic acid.

same buffer and containing the same concentration of ligand. The volume introduced was checked by weighing. The cuvette was stoppered and its contents were mixed with a glass-covered magnetic stirrer bar which remained in the cuvette. The spectrum was recorded using as reference either buffer alone or buffer containing the test ligand at the same concentration as the sample (16 μM unless otherwise indicated). Additions were repeated until further increases in nucleic acid concentration failed to alter the spectrum detectably. Losses of solvent due to evaporation were less than 0.5% during each titration. The concentration of drug bound to nucleic acid, c_b, and free in solution, c_f, was calculated from the absorbance change at each nucleic acid concentration (19, 20). Absorbances at or near the maximum in the difference spectrum were used after correction for the slight contribution of the nucleic acid solution in the visible region (apparent molar extinction coefficient at 410 nm typically about 10).

Calculation of binding parameters: equilibrium dialysis and spectrophotometric titrations. Binding parameters were determined using the model of McGhee and Von Hippel (21), which takes into account the effects of neighboring site exclusion in binding of ligands to a 1-dimensional homogeneous lattice. In this model the binding curve is described by the equation

$$r/c_f = K(1 - nr)\left[\frac{1 - nr}{1 - (n-1)r}\right]^{n-1} \quad (1)$$

where r is the binding ratio (ligand bound per lattice unit), c_f is the free drug concentration, K is the intrinsic association constant, and n is the site size (lattice units occluded by one bound ligand). This model therefore predicts curvature of Scatchard plots (plots of r/c_f versus r) even in the absence of site heterogeneity or ligand-ligand cooperativity. Values of K and n giving best fit to the data were determined by computer using an iterative FORTRAN program written by Dr. J. D. McGhee, Laboratory of Molecular Biology, National Institutes of Health, Bethesda, Md.

It should be noted that the McGhee-Von Hippel model differs in an important respect from the Scatchard model (22): K is defined with respect to the lattice unit, not the total binding site which embrances adjacent excluded lattice units. The values of K (and, to a lesser extent, n) determined from binding data depend critically on the choice of lattice unit, which must be defined such that the concentration of lattice units corresponds to the concentration of potential sites when $r = 0$. For this reason we have chosen a lattice unit of one base pair for binding of these intercalating drugs to native DNA, whereas on the basis of data presented below a lattice unit of one nucleotide has been assumed to be more appropriate for heat-denatured DNA or RNA. Therefore, Eq. 1 was fitted to experimental data with r expressed in base pairs for native DNA and in nucleotides for the single-stranded polymers.

Ethidium displacement method and calculation of binding constants. Values of C_{50}, defined as the concentration of drug required to halve the observed fluorescence due to DNA-bound ethidium, were determined as previously described (23) in SHE buffer with 1 μM DNA and 1.26 μM ethidium. Fluorescence may be reduced by either displacement or quenching of fluorescence of DNA-bound ethidium (11). Quenching was determined in a separate assay and used to calculate the true extent of ethidium displacement at the critical (C_{50}) drug concentration (24). The degree of quenching varied with the drug and DNA used, and in general was greatest for *m*-AMSA and least for 9-AA, 9-Me-AA, and proflavine. The ethidium displacement data were used to estimate association constants employing a competition model based on the generalized form of equation 10 described by McGhee and Von Hippel (21). It was assumed that drug and ethidium compete for the same DNA binding sites and that the binding of each is subject to neighboring-site exclusion (i.e., $n = 2$ in Eq. 1). The magnitude of

TABLE 2

Spectral parameters of the nucleic acid complexes of AMSA drugs and 9-AA in SHE buffer

Ligand	Native DNA			Denatured DNA			TYMV RNA		
	λ_i[a]	λ_m[b]	$10^{-3} \times \Delta\epsilon$[c]	λ_i[a]	λ_m[b]	$10^{-3} \times \Delta\epsilon$[c]	λ_i[a]	λ_m[b]	$10^{-3} \times \Delta\epsilon$[c]
	nm	*nm*	$M^{-1}\ cm^{-1}$	*nm*	*nm*	$M^{-1}\ cm^{-1}$	*nm*	*nm*	$M^{-1}\ cm^{-1}$
m-AMSA	—	412	5.24	463	412	5.10	457	412	3.84
		432	4.76		432	4.53		432	3.26
o-AMSA	—	412	4.40	—	412	4.10	—	412	3.50
		432	4.90		432	4.53		432	4.20
AMSA	—	412	4.61	—	412	4.85	—	412	3.56
		432	4.96		432	5.10		432	3.60
9-AA	428	379	3.65	428	379	3.96	428	379	3.47
		398	5.76		398	5.90		398	4.97
		420	4.42		420	4.68		420	4.04
		433	−1.79		433	−2.01		433	−1.72

[a] Wavelength of isosbestic point.

[b] Wavelength of maxima in the free drug-bound difference spectrum.

[c] Differential molar extinction coefficient at λ_m, i.e., $\epsilon_{\text{free ligand}} - \epsilon_{\text{bound ligand}}$.

fluorescence quenching was greatest with the combination of *m*-AMSA and poly(dA-dT); in this instance quenching and displacement contributed almost equally to the observed reduction of ethidium fluorescence. As a result the correction for quenching reduced the estimate of *K* approximately 4-fold. A full account of the methods and assumptions involved is published elsewhere (24). The estimated standard deviation involved in these determinations of *K* was approximately ± 20%.

Measurement of thermal denaturation of DNA. A solution containing calf thymus DNA (84 μM) in SHE buffer was placed in a cuvette (10-mm path length) with a tightly fitting Teflon stopper. The cuvette was heated in a Cary Model 15 recording spectrophotometer by circulating water from a Haake unit set at a low heating rate. The water jacket of the spectrophotometer was modified by the introduction of copper sheeting to improve thermal contact with the cuvette, and by the insulation of all exposed surfaces of the jacket with plastic foam. The temperature inside the cuvette was monitored by using a thermocouple in contact with the solution. The absorbance at 260 nm was measured over the range 25–90°, with a heating rate of 0.3–0.5°/min. Chromatography on silica gel thin layers (25) after heating indicated no detectable decomposition of drugs in the course of these experiments.

RESULTS

Spectral changes induced by nucleic acids. Addition of native calf thymus DNA to solutions of *m*-AMSA caused a bathochromic shift of 8 nm and a decrease in the extinction coefficient at all wavelengths above 350 nm. The difference spectrum displayed two maxima, at 412 and 432 nm. Addition of denatured DNA or TYMV RNA caused similar spectral changes (Table 2). The spectral perturbation induced by nucleic acids was different from that observed on titration of the acridine ring nitrogen atom by elevation of the pH above 7.0, which generated isosbestic points at 398 and 458 nm with lower absorption for the free base than the cation between these wavelengths.[4] Thus the spectral change associated with binding to nucleic acids is not a simple consequence of displacement of the acid-base equilibrium by selective binding of the cation (or neutral species).

The series of spectra generated by addition of varying quantities of calf thymus DNA (or other nucleic acids) to 9-AA generated a well-defined isosbestic point at 428 nm (Table 2). Isosbestic points were also observed for the titration of denatured DNA or TYMV RNA with *m*-AMSA (Table 2), but in other instances lack of spectral crossover between bound and free ligand precluded the use of this criterion for the existence of a single, spectrally distinct bound form. However, in all cases normalization of the difference spectrum for bound versus free drug revealed no systematic variation during the titration. Thus the assumption that the spectral characteristics of bound ligand are independent of binding ratio, a precondition for extraction of bound ligand concentrations from such data, appears to be warranted.

Binding curves. Binding isotherms for the interaction between *m*-AMSA and nucleic acids at 0.01 ionic strength are presented in Fig. 2 in the form of Scatchard plots. Although the data for binding to native DNA were analyzed in terms of base pairs as the lattice units (see Materials and Methods), in this and all subsequent figures *r* is expressed in terms of nucleotides in order to facilitate comparison with data for denatured DNA and RNA. Results obtained by both equilibrium dialysis and spectrophotometric titration are shown, but the curves have been fitted to the equilibrium dialysis data alone, since these are the more complete and extensive. The fit provided by the neighbouring site exclusion model appears to be acceptable in all cases.

It is immediately apparent that *m*-AMSA is highly selective for binding to native DNA. Its affinity for heat-denatured DNA and for RNA is calculated to be lower by factors of 5 and 25, respectively (Table 3).

Comparable results for the other three AMSA drugs are shown in Figs. 3 and 4, together with data for three simpler aminoacridines in Figs. 4 and 5. The capacity to discriminate between DNA and RNA (in favor of the former) seems to be shared by all the compounds, although it is most marked with the tumor-active drugs *m*-AMSA and AMSA (Table 3). Likewise, all of the drugs

[4] Spectrophotometric determination of pK_a proved impractical because of the extreme insolubility of the free base which precipitated rapidly at pH 7.5 or above. However, an aqueous pK_a of approximately 7.8 for *m*-AMSA has been estimated on the basis of spectrophotometric titrations in water-DMSO mixtures (G. Atwell, personal communication).

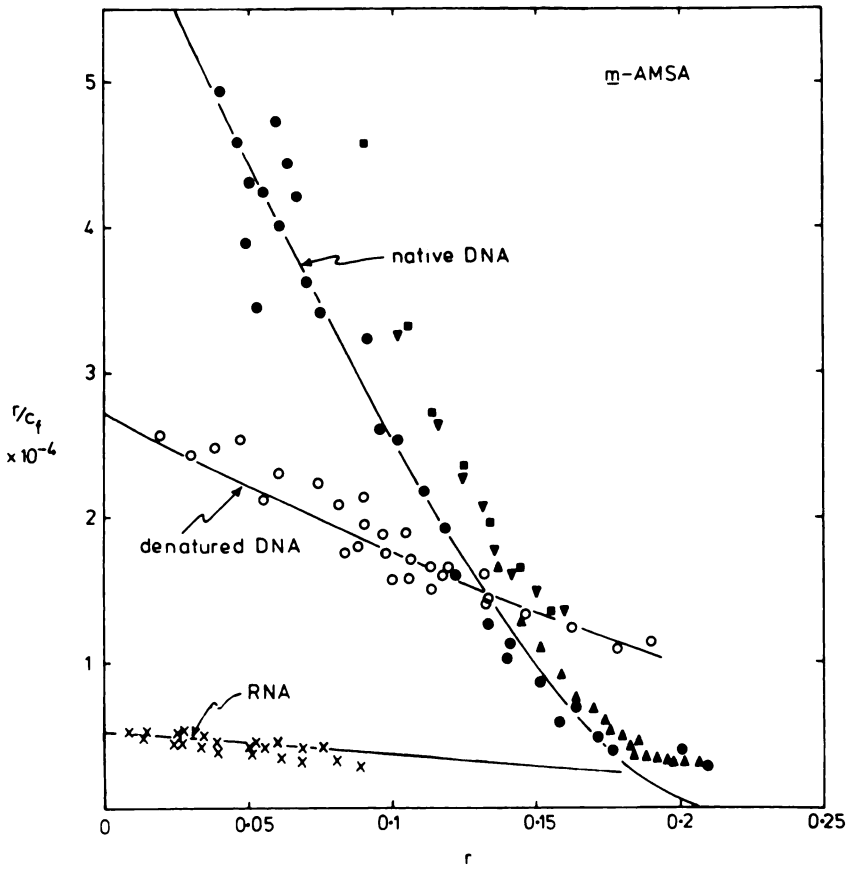

FIG. 2. *Scatchard plots for the interaction of m-AMSA with nucleic acids, ionic strength 0.01 M*

Data were obtained by equilibrium dialysis (●, native DNA; ○, denatured DNA; ×, rRNA) or spectrophotometry (■, ▼, ▲, native DNA, total ligand concentration 16, 20, and 80 μM, respectively). *r*, bound ligand per nucleotide. The curves are theoretical, representing a best fit of the equilibrium dialysis data to the model described by Eq. 1 using the values of *K* and *n* listed in Table 3.

bind better to native DNA than to denatured DNA (except 2-Me-AMSA). Another feature common to all of the 9-substituted acridines is a strong preference for denatured DNA as opposed to RNA, although both types of single-stranded polynucleotides presumably adopt much the same sort of conformation. This is not the case for proflavine, which binds slightly better to RNA than to heat-denatured DNA under these conditions (Fig. 4).

Binding to native DNA. Binding parameters defined by the curves fitted to the data for native DNA in Figs. 2–5 indicate site sizes close to two base-pairs ($n = 4$ nucleotides), as expected for the neighboring-site exclusion model. They also show that proflavine binds with a higher association constant than do the 9-aminoacridines, whereas *m*-AMSA and 2-Me-AMSA bind with the lowest affinity (Table 3). There is clearly no simple correlation between antitumor potency or selectivity and the strength of DNA binding among the seven compounds examined.

Although less extensive, data obtained by spectrophotometric titration agree reasonably well with the equilibrium dialysis results for *m*-AMSA (Fig. 2), *o*-AMSA, and AMSA (Fig. 3), and provide similar estimates of *K* and *n* when analyzed using Eq. 1 (Table 3). In the case of 9-AA, agreement is less satisfactory (Fig. 5), although since different buffers were used in the two types of assay, and since both methods are subject to potential systematic errors, the discrepancy is not alarming.

Association constants for calf thymus DNA were also determined by an ethidium competition technique (24) using the association constant for binding of ethidium to DNA at ionic strength 0.01 determined by Gaugain *et al.* (26). The results (Table 3) are in satisfactory agreement with those obtained by the other two methods. This technique is well-suited to the investigation of drug binding to synthetic polynucleotides since, subject to certain assumptions as described by Baguley *et al.* (24), association constants can be estimated using only microgram quantities of nucleic acid. This approach was therefore employed to derive association constants for the interaction between the various acridine derivatives and six synthetic DNAs (Table 4) for which ethidium binding constants in SHE buffer have previously been determined (11). The results reveal marked variations in the apparent strength of binding to polymers of different sequence. The three alternating pyrimidine·purine polymers yielded higher association constants than seen with any of the polypyrimidine·polypurine DNAs. It should be noted that each of the alternating copolymers contains two types of intercalation sites, but the individual binding constants for these sites cannot be deduced from the present results. Binding to poly(dA-dT), within experimental error, appears to be the same as binding to poly(dG-dC) for all drugs except possibly 2-Me-AMSA. Other data (not shown) suggest that a number of other 2-substituted AMSA derivatives also bind more tightly

TABLE 3

Association constant and site size (in nucleotides) for binding to nucleic acids

Binding parameters were evaluated using data of Figs. 2–5 with the lattice unit expressed in base pairs (native DNA) or nucleotides (denatured DNA and RNA), using Eq. 1.

Ligand	Method	Native DNA		heat-denatured DNA		rRNA	
		K	*n*	K	*n*	K	*n*
		M^{-1}		M^{-1}		M^{-1}	
m-AMSA	Equilibrium dialysis	1.3×10^5	4.5	2.7×10^4	2.3	5.2×10^3	2.0
	Spectrophotometry	1.8×10^5	4.3				
	Ethidium displacement	1.4×10^5	—				
o-AMSA	Equilibrium dialysis	4.0×10^5	4.1	4.8×10^4	2.8	1.8×10^4	4.3
	Spectrophotometry	3.2×10^5	3.7	3.9×10^4	1.8		
	Ethidium displacement	3.5×10^5	—				
AMSA	Equilibrium dialysis	5.5×10^5	4.3	8.7×10^4	2.6	1.4×10^4	3.0
	Spectrophotometry	3.2×10^5	3.5	9.3×10^4	2.5		
	Ethidium displacement	4.2×10^5	—				
2-Me-AMSA	Equilibrium dialysis	1.4×10^5	3.4	8.5×10^4	2.5	2.7×10^4	2.3
	Ethidium displacement	1.9×10^5	—				
9-AA	Equilibrium dialysis	3.0×10^5	4.1	9.2×10^4	2.4	3.1×10^4	2.6
	Spectrophotometry	5.3×10^5	3.7	8.2×10^4	2.0		
	Ethidium displacement	3.9×10^5	—				
9-Me-AA	Equilibrium dialysis	3.5×10^5	4.9	8.1×10^4	2.4	2.5×10^4	2.4
	Ethidium displacement	4.2×10^5	—				
Proflavine	Equilibrium dialysis	1.0×10^6	4.1	2.0×10^5	2.3	2.6×10^5	3.6
	Ethidium displacement	7.9×10^5	—				

to poly(dG-dC) than to poly(dA-dT). The results calculated for the complementary homopolymer pairs indicate tighter drug binding to poly(dG)·poly(dC) than to poly(dA)·poly(dT). It is of interest to note that the logarithmic mean of the association constants listed in Table 4 for a given drug lies close to the value obtained for calf thymus DNA (Table 3), as if the value measured for the natural DNA might represent a mean averaged

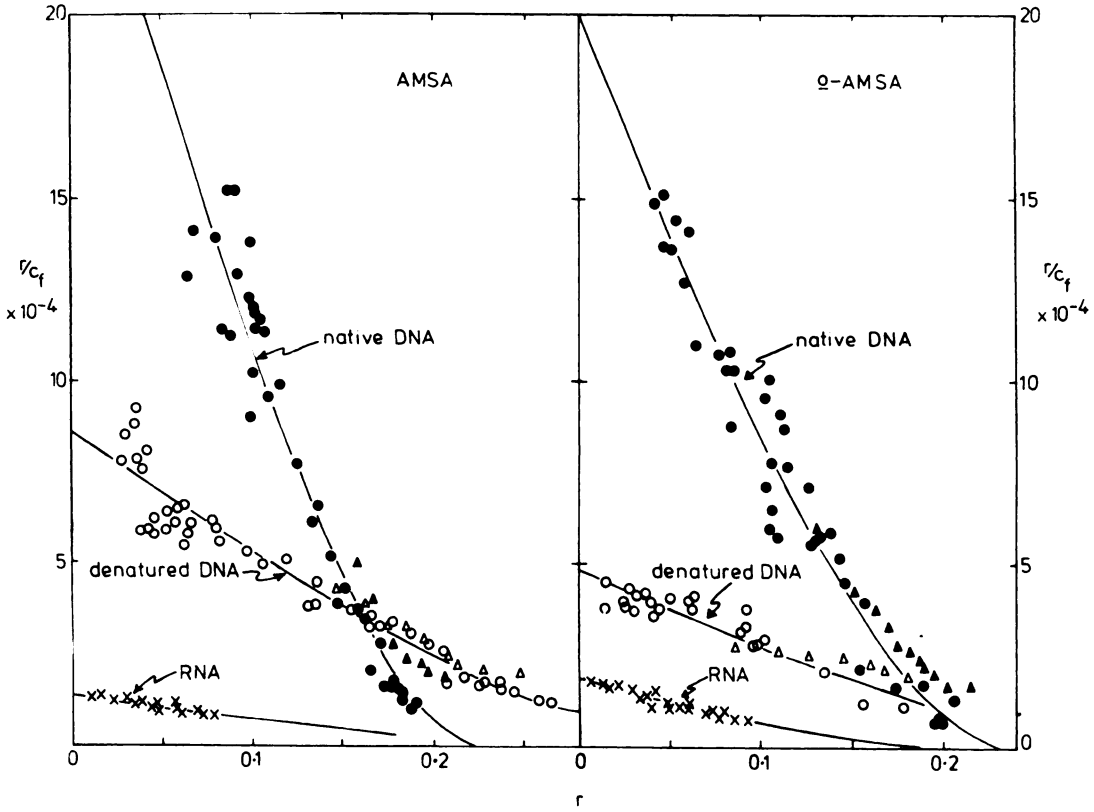

FIG. 3. *Scatchard plots for the interaction of AMSA (left panel) and o-AMSA (right panel) with nucleic acids, ionic strength 0.01 M*

Symbols as for Fig. 2, and △, spectrophotometric titration, denatured DNA. Spectrophotometric data were not included in the curve-fitting procedure.

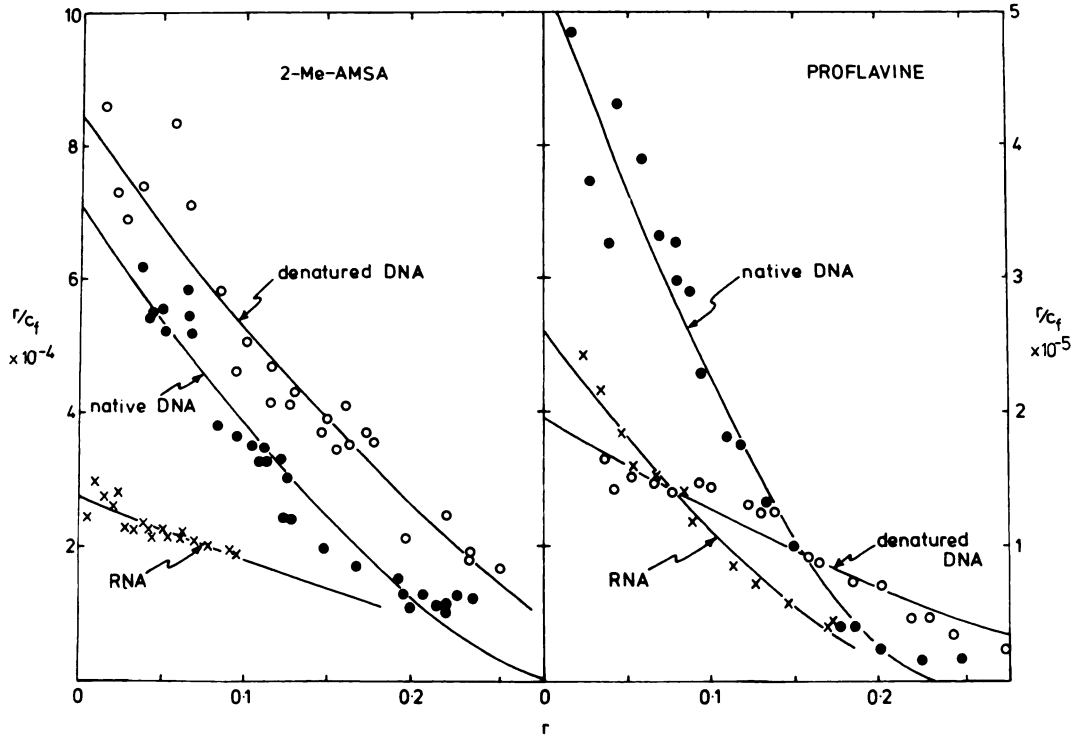

FIG. 4. *Scatchard plots for the interaction of 2-Me-AMSA (left panel) and proflavine (right panel) with nucleic acids, ionic strength 0.01* M
Symbols as for Fig. 3.

over the microscopic constants for all the sequences contained within it.

Raising the ionic strength by addition of ammonium fluoride to MAF buffer or sodium chloride to SHE buffer caused a marked decrease in the association constant for binding of *m*-AMSA to DNA (Fig. 6). A linear relationship (slope 1.1) was found to exist between log *K* and the log of the ionic strength (*inset*). Although the site size was not well-defined by these data, the fitted curves *A*, *B*, and *C* of Fig. 6 correspond to site sizes of 2.0, 1.8, and 1.5 base pairs, respectively, compared with 2.2 at ionic strength 0.01 (Table 3), suggesting that site size is not significantly dependent upon ionic strength. Similarly, the association constant for *o*-AMSA in SHE buffer as determined by spectrophotometry was decreased from 3.2×10^5 to 2.9×10^4 M^{-1} by elevation of ionic strength from 0.01 to 0.1, without a change in site size (data not shown).

Binding to heat-denatured DNA and RNA. The interaction of AMSA drugs and other acridines with heat-

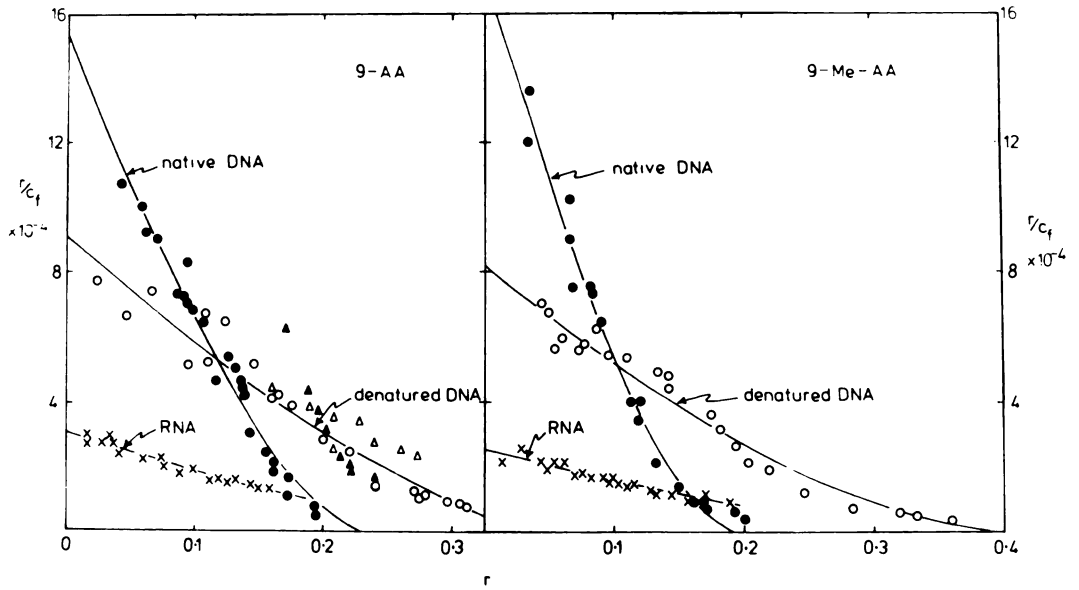

FIG. 5. *Scatchard plots for the interaction of 9-AA (left panel) and 9-Me-AA (right panel) with nucleic acids, ionic strength 0.01* M
Symbols as for Fig. 3. Spectrophotometric data were not included in the curve-fitting procedure.

TABLE 4

Calculated drug-nucleic acid association constants based on ethidium displacement in SHE buffer

Nucleic acid	$10^{-5} \times K$						
	m-AMSA	*o*-AMSA	AMSA	2-Me-AMSA	9-AA	9-Me-AA	Proflavine
				M^{-1}			
poly(dA-dT)	2.9	13	15	4.6	12	13	25
poly(dA)·poly(dT)	0.36	0.87	1.0	1.1	1.6	2.0	7.1
poly(dG-dC)	2.6	12	13	7.4	14	15	22
poly(dG)·poly(dC)	2.3	5.6	7.5	3.8	3.1	5.2	8.1
poly(dA-dC)·poly(dG-dT)	3.5	10	9.1	5.0	13	14	27
poly(dA-dG)·poly(dC-dT)	0.61	1.2	1.4	0.63	0.92	1.3	3.4

denatured calf thymus DNA in MAF buffer was investigated using equilibrium dialysis (Figs. 2–5). Spectrophotometric titrations in 0.01 SHE buffer provided data in good agreement for three ligands studied using this technique (Figs. 3 and 5). In the case of *m*-AMSA, binding was weaker, so that it proved impossible to evaluate K reliably by the spectrophotometric method.

It is evident from the data in Figs. 2–5 that denaturation increased the number of binding sites available to each drug. It was therefore clear that binding could not be restricted to residual double-stranded regions in the denatured polymer. For this reason the binding data for denatured DNA were analyzed using a lattice unit of one nucleotide (i.e., it was assumed that each nucleotide, rather than each nucleotide pair, provides one potential binding site in the naked lattice). This approach indicated that the number of binding sites increased by a factor of approximately 2 upon denaturation, and that K decreased markedly (3 to 10-fold) for all ligands with the exception of 2-Me-AMSA (Table 3).

Binding to rRNA, again analyzed assuming a lattice unit of one nucleotide, was weaker than to denatured DNA for each drug with the exception of proflavine, for which a small increase in K was observed (Table 3). Spectrophotometric titrations of *m*-AMSA, *o*-AMSA, AMSA, and 9-AA with a single-stranded viral RNA, TYMV RNA (data not shown), also revealed weaker interaction than with denatured calf thymus DNA, but with the exception of 9-AA ($K = 2.30 \times 10^4$ M^{-1}) binding was too weak to allow meaningful determination of association constants. Although K and n could not be determined, over-all binding was greatest for 9-AA, lowest for *m*-AMSA, and intermediate for *o*-AMSA and AMSA, in qualitative agreement with the equilibrium dialysis results for rRNA (Table 3).

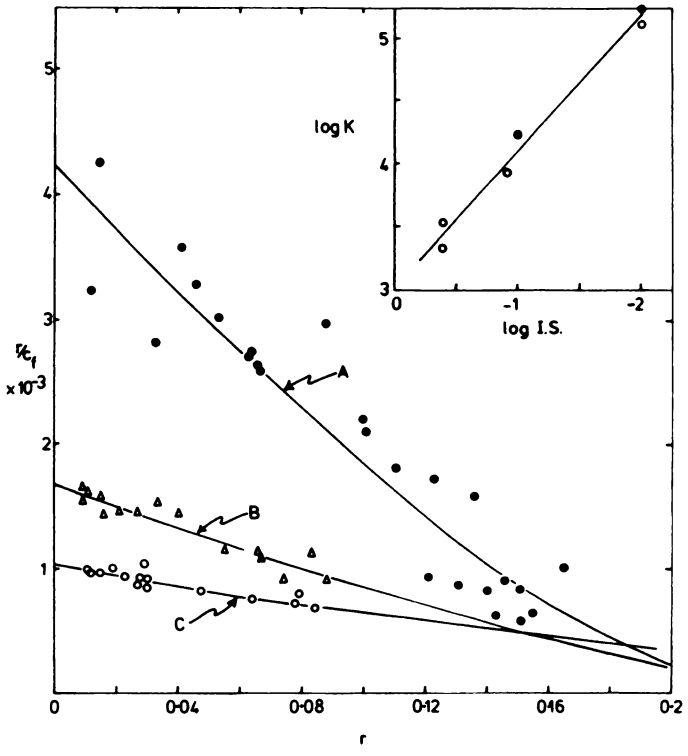

FIG. 6. *Effect of ionic strength (I.S.) on the binding of m-AMSA to native calf thymus DNA*

The Scatchard plots were determined by equilibrium dialysis using ionic strengths of 0.125 (●, *curve A*) or 0.4 M at pH 6.0 (○, *curve C*), or 0.4 M at pH 6.5 (△, *curve B*).

Inset. Plot of $\log_{10}K$ versus $\log_{10}$I.S. for the equilibrium dialysis results (○) and for data obtained by spectrophotometric titration (●).

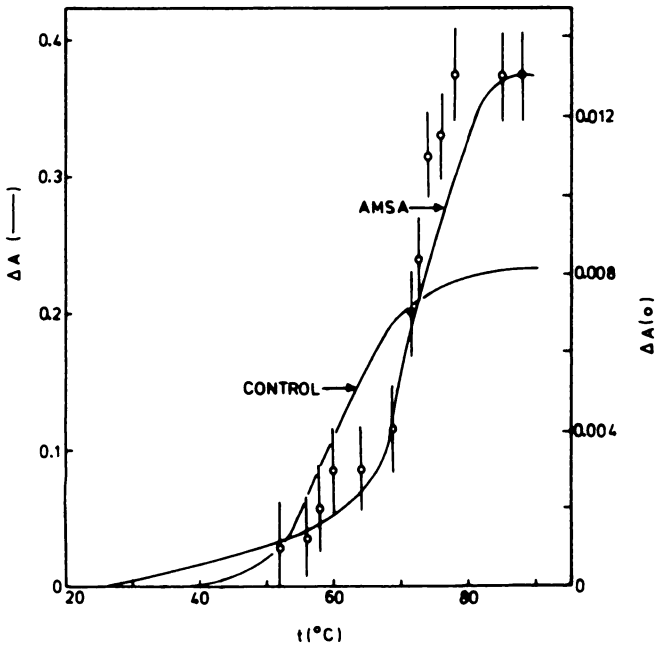

FIG. 7. *Effect of AMSA on the thermal denaturation of DNA*

Continuous curves represent the absorbance change at 260 nm (*left ordinate*) of 84 μM calf thymus DNA in SHE buffer without drug (control) or in the presence of 20 μM AMSA. Symbols (○) represent the absorbance change at 432 nm (*right ordinate*) for the solution containing AMSA. *Vertical bars* are estimated uncertainties.

Effects on thermal denaturation of DNA. In order to examine the effects of AMSA drugs on the stability of the DNA double helix, the helix-coil transition was observed by measuring the UV absorbance in the temperature range 25–90°. The midpoint of the transition was shifted to higher temperatures by the drugs (Fig. 7), attributable to stabilization of the helix. However, the total absorbance change was greater in the presence of the drugs than in the control (Fig. 7). Since the DNA-drug complexes had lower UV absorption at room temperature than the sum of the absorbance of free drugs plus DNA, a component of the hyperchromicity at 260 nm could be contributed by the displacement of drug from the DNA at elevated temperatures. That such displacement occurs with AMSA was confirmed by monitoring the transition at the maximum of the free drug-complex difference spectrum in the visible range (432 nm). The expected slight hyperchromicity was observed (Fig. 7). Under conditions in which a large proportion of the observed hyperchromicity at 260 nm is due to drug displacement, the temperature at the midpoint in the absorbance profile ($T_{1/2}$) need not correspond to that at the true midpoint of the helix-coil transition (T_m). However, the displacement of AMSA drugs as detected by the hyperchromicity at 432 nm appeared to occur concomitantly with the hyperchromic transition in the ultraviolet (Fig. 7). The measured $T_{1/2}$ must therefore correspond to T_m within the limits of experimental error.

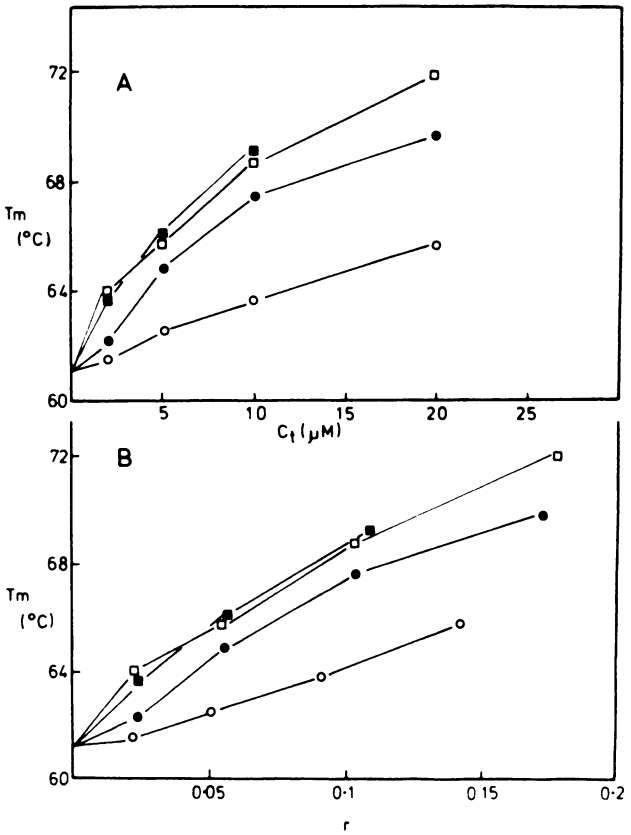

FIG. 8. *Effects of AMSA drugs and 9-AA on the T_m of native calf thymus DNA*

The T_m was related to the total ligand concentration, C_t, in *panel A*, and to the binding ratio at 25° (r, bound ligand per nucleotide) in *panel B* using the spectrophotometric data of Table 3. ○, *m*-AMSA; ●,*o*-AMSA; □, AMSA; ■, 9-AA.

Values of T_m were measured for DNA in the presence of varying concentrations of drugs (Fig. 8A). All of the agents caused significant elevation of T_m, the effect increasing with drug concentration in the range studied. AMSA and 9-AA had the greatest effect on T_m, with *o*- and *m*-AMSA showing progressively less effect. The T_m of the drug-DNA complexes was related to the binding ratio at 25° by solving Eq. 1 for r using the values of K and n listed in Table 3. The data for the four compounds did not reduce to a single curve (Fig. 8B), indicating that the extent of binding at room temperature was not the only factor influencing T_m.

DISCUSSION

For ligands such as intercalating drugs, which are subject to neighboring-site exclusion effects, binding parameters cannot be determined by the traditional method of Scatchard (22), since the total number of binding sites (free and occupied) is not independent of the binding ratio.

The procedure adopted here, which follows the method of McGhee and Von Hippel (21), is one of several (27–29) which allow for the effect of neighboring-site exclusion. This model appears to account satisfactorily for the curvature of the plots shown in Figs. 2–6. However, in contrast to the Scatchard treatment, binding parameters in the McGhee-Von Hippel model are critically dependent upon the choice of lattice unit. For intercalating agents such as AMSA drugs and simple aminoacridines, it is reasonable to assume that the concentration of potential binding sites in the naked lattice (S_o) corresponds to the concentration of interbase-pair regions in double-stranded DNA. Consequently we have approximated S_o as the concentration of base pairs and have expressed binding ratios accordingly. Although in the Scatchard model the choice of lattice unit is arbitrary, the analysis of binding data using Eq. 1 with r expressed in nucleotides rather than base pairs would reduce the estimate of K by a factor of approximately 2 and lower the value of n by approximately 10%.

The observed correspondence between association constants determined by equilibrium dialysis, spectrophotometry, and ethidium displacement strengthens confidence in the estimated binding parameters and tends to validate the applicability of the ethidium displacement method in these experiments. The latter approach provides a convenient method for the rapid investigation of binding to double-stranded polynucleotides, including those whose cost precludes their use in other assays for drug binding. By this means we have been able to detect marked variations in apparent association constants for different potential intercalation sites for each drug studied (Table 4). Since these results imply that calf thymus DNA cannot be considered a homogeneous lattice, we cannot exclude the possibility that significant ligand-ligand cooperativity is being masked by site heterogeneity over the range of r which appears to be acceptably fitted by the simple neighboring-site exclusion model.

The ionic strength dependence of the binding of *m*-AMSA to native DNA (Fig. 6) is in good agreement with the prediction of Record *et al.* (30) for a monocationic compound. These workers predicted the logarithm of the association constant to be linearly related to the loga-

rithm of the ionic strength with a proportionality constant close to 1.

Examination of the association constants listed in Table 3 suggests that the methanesulfonanilide ring of AMSA drugs does not interfere with binding to double-stranded DNA, since AMSA and *o*-AMSA bind with affinity similar to that of 9-AA or 9-Me-AA. This conclusion is consistent with earlier studies demonstrating that sterically demanding substituents at position 9 of the acridine nucleus do not prevent DNA binding (20). Studies with space-filling molecular models suggest that the methanesulfonanilide moiety of AMSA can be located in the minor groove of B-DNA [i.e., with an orientation analogous to that accepted for ethidium (31)] without interfering with intercalation by the acridine nucleus when the conformation of the drug is as established by X-ray crystallography (13). The 2′-OCH_3 group present in *o*-AMSA is not likely to impede this interaction either, but in the case of *m*-AMSA the 3′-OCH_3 group limits the extent to which the acridine nucleus can be made to overlap the base pairs. This steric hindrance to intercalation may account for the lower association constant for *m*-AMSA (Table 3) as well as the relative inability of this ligand to stabilize double-stranded DNA against thermal denaturation (Fig. 7). Other AMSA derivatives with sterically demanding 3′-substituents (Me, $NHSO_2CH_3$, NO_2, Cl, OH) also display reduced affinity for double-stranded DNA.[5] Steric factors may also be responsible for the weak binding of 2-Me-AMSA, since in our model accommodation of the 2-methyl group would require a change in the orientation of the acridine nucleus within the intercalation site, thus bringing the 3′-position of the methanesulfonanilide ring into close contact with base pairs in the minor groove. Such interactions could again impede optimal ring overlap. Support for this hypothesis can be drawn from the observation that the unwinding angle of intercalated 2-Me-AMSA is significantly lower than that for AMSA, *m*-AMSA, or *o*-AMSA (12), consistent with an altered acridine ring orientation.

Denaturation of DNA caused a decrease in *K*, together with an approximately 2-fold increase in the number of sites available, as noted in previous studies with acridines (32). This result contrasts with that for certain other intercalating drugs such as echinomycin, where binding to denatured DNA appears to be restricted to residual double-stranded regions (33). The estimated site sizes (Table 3) close to two nucleotides would be consistent with intercalation of the acridine moiety between adjacent bases in single-stranded polymers, possibly in a fashion similar to that of the asymmetric 9-AA:iodocytidylyl-(3′, 5′)-guanosine complex (34), with neighboring-site exclusion. Lack of information on the conformation of single-stranded polynucleotides precludes speculation as to the likely stereochemical basis of any such exclusion.

The present study has not revealed any straightforward correlation between nucleic acid binding parameters and antitumor activity for four members of the AMSA series. Thus *m*-AMSA binds to nucleic acids with lower affinity than does the tumor-inactive positional isomer *o*-AMSA or the parent compound AMSA, which is an active antitumor agent with lower molar potency. On the other hand, our continuing studies on a more extensive series of 9-anilinoacridine drugs (35, 36) do reveal a positive correlation between affinity for DNA and antitumor activity, but suggest that the effects of the 1′-methanesulfonamide and 3′-methoxy ring substituents on antitumor activity are mediated by mechanisms other than gross DNA binding. Our present hypothesis based on these findings is that the biological action of AMSA drugs is exerted through the formation of ternary complexes in which the acridine moiety serves as the DNA-binding anchor whereas the methanesulfonanilide ring interacts with a second macromolecular species. Quantitative structure-activity relationships have demonstrated a requirement for a high electron density at the 6′-position of the anilino ring (4), a condition which is fulfilled in *m*-AMSA but not in *o*-AMSA. Interaction of this electron-rich center with critical chromosomal proteins could be responsible for the cytotoxic effects of AMSA compounds at the very low binding ratios likely to be encountered in the cell.

[5] B. C. Baguley, unpublished data.

ACKNOWLEDGMENTS

We thank Dr. J. D. McGhee and the late Professor B. F. Cain for helpful discussions and suggestions during the course of the study.

REFERENCES

1. Cain, B. F., and G. J. Atwell. The experimental antitumour properties of three congeners of the acridylmethanesulphonanilide (AMSA) series. *Eur. J. Cancer* **10**:539–549 (1974).
2. Rozencweig, M., D. D. von Hoff, R. L. Cysyk, and F. M. Muggia. *m*-AMSA and PALA: two new agents in cancer chemotherapy. *Cancer Chemother. Pharmacol.* **3**:135–141 (1979).
3. Legha, S. S., G. R. Blumenschein, A. U. Buzdar, G. N. Hortobagyi, and G. P. Bodey. Phase II study of 4′-(9-acridinylamino)methanesulfon-*m*-anisidide (AMSA) in metastatic breast cancer. *Cancer Treat. Rep.* **63**:1961–1964 (1979).
4. Cain, B. F., G. J. Atwell, and W. A. Denny. Potential antitumor agents. 16. 4′-(Acridin-9-ylamino)methanesulfonanilides. *J. Med. Chem.* **18**:1110–1117 (1975).
5. Denny, W. A., G. J. Atwell, and B. F. Cain. Potential antitumour agents. 32. Role of agent base strength in the quantitative structure-antitumor relationships for 4′-(9-acridinylamino)methanesulfonamide analogues. *J. Med. Chem.* **22**:1453–1460 (1979).
6. Wilson, W. R. Studies on the mode of action of the antitumour acridine 4′-(9-acridinylamino)methanesulphon-*m*-anisidide (*m*-AMSA). Ph.D. thesis, University of Auckland (1978).
7. Tobey, R. A., L. L. Deaven, and M. S. Oka. Kinetic response of cultured Chinese hamster cells to treatment with 4′-[(9-acridinyl)-amino] methanesulphon-*m*-anisidide-HCl. *J. Natl. Cancer Inst.* **60**:1147–1153 (1978).
8. Furlong, N. B., J. Sato, T. Brown, F. Chavez, and R. B. Hurlbert. Induction of limited DNA damage by the anti-tumor agent Cain's acridine. *Cancer Res.* **38**:1329–1335 (1978).
9. Deaven, L. L., M. S. Oka, and R. A. Tobey. Cell-cycle-specific chromosome damage following treatment of cultured Chinese hamster cells with 4′-[(9-acridinyl)-amino]methanesulphon-*m*-anisidide-HCl. *J. Natl. Cancer Inst.* **60**: 1155–1161 (1978).
10. Gormley, P. E., V. S. Sethi, and R. L. Cysyk. Interaction of 4′-(9-acridinylamino)methanesulfon-*m*-anisidide with DNA and inhibition of oncornavirus reverse transcriptase and cellular nucleic acid polymerases. *Cancer Res.* **38**: 1300–1306 (1978).
11. Baguley, B. C., and E. M. Falkenhaug. The interaction of ethidium with synthetic double-stranded polynucleotides at low ionic strength. *Nucleic Acids Res.* **5**:161–171 (1978).
12. Waring, M. J. DNA-binding characteristics of acridinylmethanesulphonanilide drugs: comparison with antitumour properties. *Eur. J. Cancer* **12**:995–1001 (1976).
13. Hall, D., D. A. Swann, and T. N. Waters. Crystal and molecular structure of 4′-(acridin-9-ylamino)methanesulphonanilide hydrochloride, a compound showing anti-leukemic activity. *J. Chem. Soc. Perkin. Trans. II* 1334–1337 (1974).
14. Cain, B. F., R. N. Seelye, and G. J. Atwell. Potential antitumor agents. 14. Acridylmethanesulfonanilides. *J. Med. Chem.* **17**:922–930 (1974).
15. Wells, R. D., J. E. Larson, R. C. Grant, B. E. Shortle, and C. R. Cantor. Physiochemical studies on polydeoxyribonucleotides containing defined repeating nucleotide sequences. *J. Mol. Biol.* **54**:465–497 (1970).

16. Mahler, H. R., B. Kline, and B. D. Mehrotra. Some observations on the hypochromism of DNA. *J. Mol. Biol.* **9**:801–811 (1964).
17. Matthews, R. E. F., and R. K. Ralph. Turnip yellow mosaic virus. *Adv. Virus Res.* **12**:273–328 (1966).
18. Müller, W., D. M. Crothers, and M. J. Waring. A non-intercalating proflavine derivative. *Eur. J. Biochem.* **39**:223–234 (1973).
19. Waring, M. J. Complex formation between ethidium bromide and nucleic acids. *J. Mol. Biol.* **13**:269–282 (1965).
20. Blake, A., and A. R. Peacocke. The interaction of aminoacridines with nucleic acids. *Biopolymers* **6**:1225–1253 (1968).
21. McGhee, J. D., and P. H. von Hippel. Theoretical aspects of DNA-protein interactions: co-operative and non co-operative binding of large ligands to a one-dimensional homogeneous lattice. *J. Mol. Biol.* **86**:469–489 (1974).
22. Scatchard, G. The attractions of proteins for small molecules and ions. *Ann. N. Y. Acad. Sci.* **51**:660–672 (1949).
23. Cain, B. F., B. C. Baguley, and W. A. Denny. Potential antitumor agents. 28. Deoxyribonucleic acid polyintercalating agents. *J. Med. Chem.* **21**:658–668 (1978).
24. Baguley, B. C., W. A. Denny, G. J. Atwell, and B. F. Cain. Potential antitumor agents. 34. Quantitative relationships between DNA binding and molecular structure for 9-anilinoacridines substituted in the anilino ring. *J. Med. Chem.* **24**:170–177 (1981).
25. Wilson, W. R., B. F. Cain, and B. C. Baguley. Thiolytic cleavage of the antitumour compound 4′-(9-acridinylamino)methanesulphon-*m*-anisidide (*m*-AMSA, NSC 156303) in blood. *Chem. Biol. Interact.* **18**:163–178 (1977).
26. Gaugain, B., J. Barbet, N. Capelle, B. P. Roques, and J. B. Le Pecq. DNA bifunctional intercalators. 2. Fluorescence properties and DNA binding interaction of an ethidium homodimer and an acridine heterodimer. *Biochemistry* **17**:5078–5088 (1978).
27. Crothers, D. M. Calculation of binding isotherms for heterogeneous polymers. *Biopolymers* **6**:575–584 (1968).
28. Zasedatelev, A. S., G. V. Gursky, and M. V. Volkenshtein. Theory of one-dimensional adsorption. I. Adsorption of small molecules on a homopolymer. *Mol. Biol.* (*Mosc.*) **5**:194–198 (1971).
29. Schellman, J. A. Co-operative multisite binding to DNA. *Isr. J. Chem.* **12**: 219–238 (1974).
30. Record, M. T., T. M. Lohman, and P. De Haseth. Ion effects on ligand-nucleic acid interactions. *J. Mol. Biol.* **107**:145–158 (1976).
31. Waring, M. J. Inhibitors of nucleic acid synthesis, in *The Molecular Basis of Antibiotic Action* (E. F. Gale, E. Cundliffe, P. E. Reynolds, M. H. Richmond, and M. J. Waring, eds.), 2nd Ed. Wiley, London, in press (1981).
32. Drummond, D. S., V. F. W. Simpson-Gildemeister, and A. R. Peacocke. Interaction of aminoacridines with deoxyribonucleic acid: effects of ionic strength, denaturation and structure. *Biopolymers* **3**:135–153 (1965).
33. Waring, M. J., and L. P. G. Wakelin. Echinomycin: a bifunctional intercalating antibiotic. *Nature* (*Lond.*) **252**:653–657 (1974).
34. Sakore, T. D., B. S. Reddy, and H. M. Sobell. Visualization of drug-nucleic acid interactions at atomic resolution. IV. Structure of an aminoacridine-dinucleoside monophosphate crystalline complex, 9-aminoacridine-5-iodocytidylyl-(3′-5′)-guanosine. *J. Mol. Biol.* **135**:763–785 (1979).
35. Baguley, B. C., W. A. Denny, G. J. Atwell, and B. F. Cain. Potential antitumour agents. 35. Quantitative relationships between antitumor (L1210) potency and DNA binding for 4′-(9-acridinylamino)methanesulfon-*m*-anisidide (*m*-AMSA) analogues. *J. Med. Chem.* **24**:520–525, (1981).
36. Robertson, I. G. C., W. A. Denny, and B. C. Baguley. Inhibition of T4 bacteriophage yield by 9-anilinoacridines; comparison with *in vivo* antitumour activity. *Eur. J. Cancer* **16**:1133–1139 (1980).

Send reprint requests to: Dr. William R. Wilson, Department of Pathology, University of Auckland School of Medicine, Private Bag, Auckland, New Zealand.